JOURNAL OF PROPULSION AND POWER
Vol. 20, No. 3, May–June 2004

Kinetic Modeling of Heptane Combustion and PAH Formation

V. I. Babushok* and W. Tsang†
National Institute of Standards and Technology, Gaithersburg, Maryland 20899

A kinetic model for high-temperature oxidation and pyrolysis of heptane has been developed. This model is based on new results for heptane decomposition, decomposition and isomerization of heptyl radicals, and decomposition of olefins and olefinic radicals. It is combined with kinetic data from Grimech-3.0 model on the reactions of C_1-C_2 species. The subset on C_3-C_4 chemistry is based on the works of Marinov et al. (1998) and Laskin et al. (2000). The database for PAH formation is based on the results from kinetic models on heptane suitably modified from various soot formation models. The model was validated against experimental data on burning velocity, ignition delays, and OH time history during heptane ignition behind shock wave. The reactions determining burning velocity were established through sensitivity analysis. The main reactions determining burning velocity of heptane are similar to the reactions determining burning velocity of C_1-C_4 hydrocarbons. The influence of product distribution of heptyl radical decomposition on PAH production was analyzed.

I. Introduction

THE aim of this work was to develop a complete kinetic model of heptane combustion including new data on the cracking of heptane. This involves the kinetics of heptane decomposition, heptyl radical decomposition and isomerization, and decomposition of olefins and olefinic radicals. The intention was to combine it with C_1-C_2 species reactions from Grimech-3.0 mechanism[‡] and the reaction subset of C_3-C_4 chemistry based on the works of Marinov et al.[1] and Laskin et al.[2] With the use of this model, we will analyze reaction pathways for polyaromatic hydrocarbon (PAH) formation during heptane combustion. The PAH reaction subset was assembled from the data bases of Marinov et al.,[1] Appel et al.,[3] Richter et al.[4] (also Richter, H., personal communication, 2002) and recent kinetic data on PAH formation from several sources.[5–7] The purpose of PAH formation modeling was to investigate in more detail the dependence of PAH formation on the product distribution from heptyl radical decomposition.

We will present two versions of the suggested kinetic model. First is the detailed kinetic model for high-temperature heptane oxidation, mentioned earlier. Analysis of the decomposition kinetics of heptyl radicals and results of high-temperature modeling of heptane oxidation demonstrates that reactions involving formation and consumption of heptyl radicals can be represented by overall processes as a result of the large reaction rates of their decomposition in comparison with other reaction processes. It was shown that temperature dependencies of branching ratios for decomposition of heptyl radicals can be represented by typical Arrhenius temperature dependence.[8] This leads to some simplification of the kinetic model and elimination of several species from the model through overall representation of heptane consumption reactions leading directly to C_1-C_6 products. Combination of these overall heptane consumption reactions with detailed kinetic model for C_1-C_6 species represents the second version of kinetic model.

We will begin with a short review of kinetic models for heptane combustion and available data on the burning velocity. Next we will describe in detail the construction of a kinetic database for heptane combustion. Comparison of modeling results with experimental data on burning velocity will be the specific target of this part. In the second part of paper, the results of kinetic modeling of PAH production during heptane combustion will be presented.

II. Background

Development of comprehensive kinetic models for the combustion of hydrocarbon fuels is of interest for detailed modeling of processes in engines and for studies of the emission of toxic combustion byproducts, soot formation, and effects of different additives on the combustion process. Modeling of heptane combustion is of particular interest. Heptane is a reference fuel for the determination of a fuel's tendency to knock. It is a liquid fuel and can undergo many of the same types of reactions as larger alkanes. Heptane represents a model fuel for the alkane component of practical fuels. As was the case with smaller hydrocarbons, there is a plethora of models with their individual databases.

A. Kinetic Models of Heptane Combustion

Earlier kinetics databases for modeling of heptane combustion are summarized in Table 1. The first kinetic model of heptane combustion was developed by Coats and Williams.[31] Comprehensive kinetic models for heptane combustion were developed by Warnatz[65] and Westbrook et al.[11] These models served as a basis for further development and improvement of kinetic mechanisms of heptane oxidation.

More recent kinetics databases of heptane combustion are discussed next. Curran et al.[13] developed a comprehensive kinetic model that included reactions important to high- and low-temperature heptane oxidation. The model is based on previous kinetic models developed by Westbrook et al.[11] Older data were brought up to date, and new classes of reactions were added. Special attention was paid to the low-temperature heptane oxidation. This is important for the modeling of negative temperature coefficient (NTC) phenomenon and cool flame oxidation. Under 900 K, the primary reaction of alkyl radicals is the addition of oxygen caused by the high activation energy of beta-scission of alkyl radicals. It was found that reactions of ketohydroperoxides are important for the modeling two-stage low-temperature ignition. Recently, Westbrook et al.[66,67] extended this model to combustion of different heptane isomers.

Seiser et al.[14] simplified the model of Curran et al.[13] for simulations of heptane ignition and combustion in counterflow, nonpremixed systems. Some modifications of rate constants (alkyl radical addition to oxygen and reactions of RO_2 radical) and thermodynamic parameters (peroxy radicals) were made. The model was validated against experimental data on ignition delays in the low temperature range and experimental data on heptane ignition in a counterflow nonpremixed system from authors' experiments.

Received 8 May 2003; revision received 27 October 2003; accepted for publication 2 November 2003.

*Research Contractor.

†Research Chemist.

‡Data available online at http://www.me.berkeley.edu/gri_mech.

Table 1 Comparison of modeling results on heptane combustion with experimental data using reference numbers

Model	Ignition delay	Burning velocity	Opposite diffusion flame	Flame structure	Stirred reactor	Flow reactor	Static reactor	Rapid compression machine
Ref. 9	——	Refs. 32, 33	——	——	——	——	——	——
Ref. 10	Refs. 34, 35	Refs. 32, 33	——	——	——	——	——	——
Ref. 11	Refs. 31, 36, 38, 39	——	——	——	——	——	Ref. 58	Refs. 26, 59–63
Ref. 12	Ref. 37	——	——	——	——	——	——	Ref. 64
Ref. 13	Refs. 31, 34, 36	——	——	——	Refs. 53, 54	Refs. 26, 57	——	Refs. 59, 61–63
Ref. 14	Ref. 34	——	Ref. 14	——	——	——	——	Ref. 59
Ref. 15	——	Ref. 33	Refs. 45–48	——	Ref. 24	——	——	——
Ref. 16	——	——	——	——	Ref. 55	——	——	——
Ref. 17	——	——	——	——	Refs. 24, 53	——	——	——
Ref. 18	——	——	——	——	Ref. 56	——	——	——
Ref. 19	——	Ref. 33	——	Refs. 19, 51	——	——	——	——
Ref. 20	——	——	——	Ref. 52	——	——	——	——
Ref. 21	Ref. 34	——	——	——	——	——	——	——
Ref. 22	——	——	Refs. 46, 49, 50	——	——	——	——	——
Ref. 23	——	——	Refs. 49, 50	——	——	——	——	——
Ref. 24	Refs. 31, 38, 39	——	——	——	Ref. 24	——	——	——
Ref. 25	Ref. 34	——	——	——	Refs. 53, 54	——	——	——
Ref. 26	——	——	——	——	——	Ref. 26	——	Ref. 26
Ref. 27	——	——	Ref. 27	——	——	——	——	——
Ref. 28	Ref. 36	Refs. 32, 33	——	——	Ref. 24	Ref. 28	——	——
Ref. 29	——	——	——	Ref. 29	——	——	——	——
Ref. 30	Ref. 39–44	——	——	——	——	——	——	——
Ref. 31	Ref. 31	——	——	——	——	——	——	——

Lindstedt and Maurice[15] assembled a heptane combustion model based on the works of Chakir et al.,[24,68,69] Dagaut et al.,[70–72] Foelsche et al.,[73] Tsang,[74,75] and Westbrook et al.[11,76] The assembled model was optimized by comparisons with experimental data from diffusion flames, combustion in stirred reactors, and premixed flames. The authors simulated the dependence of burning velocity on the equivalence ratio. It was indicated that the modeling results agree with the experimental values determined by Gibbs and Calcote,[33] but for rich flames the computed values of the burning velocity were too high in comparison with the experimental data.

Bakali et al.[19] developed a heptane kinetic database for the analysis of heptane flame structure. The mechanism was based on a previously developed kinetic model for the combustion of rich acetylene-oxygen-argon flame. Simulated burning velocities of n-heptane-air mixtures at 298 K were compared with experimental data of Gibbs and Calcote.[33] The authors indicated that the maximum burning velocity was in reasonable agreement. However, overprediction for rich mixtures in comparison with experimental data was also observed.

B. Experimental Data

Experimental data on heptane combustion cover measurements of ignition delays; experiments in jet stirred, static, and plug flow reactors; and measurements of concentration and temperature profiles for laminar premixed and opposed flow diffusion flames, burning velocity determinations, measurements in rapid compression machines, and measurements in shock tubes. Data cover overall process characteristics (burning velocity, ignition delay, overall reaction rate, effective activation energy, extinction strain rate) and detailed characteristics of heptane oxidation (flame structure, concentrations for stirred and plug flow reactors). Table 1 contains a summary of the separate models and the various experimental data used for validation of these models.

There is a general tendency to cover only a limited set of experimental results. The earlier studies can be grouped in terms of two different types of applications. The first involves the simulation of high-temperature behavior and is applicable to premixed and diffusion flames. A second group of studies cover the simulation of lower-temperature behavior (cool flames, two-stage ignition, negative temperature coefficient) and the related phenomenon—engine knock. Division of models between high- and low-temperature models is limited. It is related to alkylperoxy radical kinetics, which is important for low and intermediate temperatures. Inclusion of alkylperoxy radical reactions leads to a substantial increase of kinetic models in the number of considered species and reactions. In general these reactions are not important for flame processes and high-temperature ignition behind shock waves (for temperatures more than 1200–1300 K). Note that models developed for simulation of low-temperature range phenomena contain reactions important for modeling of high-temperature kinetics, for example, a recent kinetic model[13] with detailed description of alkylperoxy radical kinetics was validated against high-temperature heptane ignition delays behind shock waves.

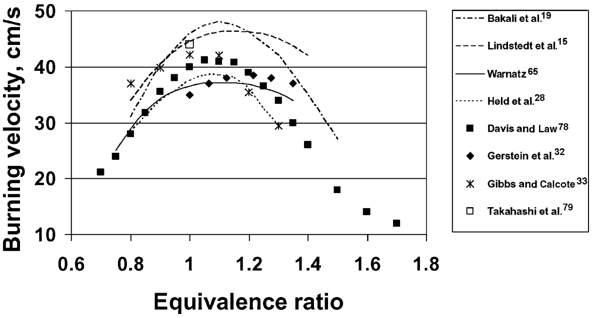

Fig. 1 Burning velocity dependence on equivalence ratio of heptane/air mixtures: ■, □, ◆, ⋇, experimental data[78,79,32,33]; ——, – – –, –·–, · · · ·, modeling results.[65,15,19,28]

The first group of models (high-temperature range) was validated against data on burning velocity, measurements for opposite diffusion flames, flame structure data, results obtained for jet stirred reactors, and measurements in shock tubes. The basis for validation of the second group of models are measurements of autoignition delays, measurements in jet stirred reactors, rapid compression machines (ignition delay), and data obtained for plug and static reactors.

C. Burning Velocity Data

Figure 1 contains available data on experimental measurements of equivalence ratio dependence of burning velocity. The early measurements of heptane burning velocity are those of Gerstein et al.,[32] Heimel and Weast,[77] and Gibbs and Calcote.[33] Recent measurements have been performed by Davis and Law[78] using the counterflow twin-flame procedure. In addition, Fig. 1 contains experimental data of Takahashi et al.[79] Babkin et al.[80] and Ryan and Leste[81] measured pressure and temperature dependencies of heptane burning velocity using a constant volume bomb procedure. Also included are the results on the calculated flame velocities.[15,19,28,65] It can be

Table 2 Kinetic models used in this work

Kinetic model	Year	Hydrocarbon
Curran et al.[13]	1998	C_7H_{16}
Seiser et al. model[14]	2000	C_7H_{16}
Reduced Seiser et al. model,[14] present work	——	C_7H_{16}
Lindstedt and Maurice model[15]	1995	C_7H_{16}
Bakali et al.[19]	1999	C_7H_{16}
Model based on Grimech-3.0,[a] present work	——	C_7H_{16}
Kinetic model of heptane combustion, present work	——	C_7H_{16}
Kinetic model of heptane combustion, including PAH formation reactions, present work	——	C_7H_{16}, PAH
Kinetic model of heptane combustion with lumped heptyl radical kinetics, present work	——	C_7H_{16}
Grimech 3.0[a]	2000	CH_4 (C_1-C_2)
Optimized C_1-C_3 model of Qin et al.[86]	2000	C_1-C_3
1,3-butadiene oxidation model of Laskin et al.[2]	2000	1,3-butadiene oxidation
Marinov et al.[1]	1998	Butane, PAH
Appel et al.[3]	2000	C_1-C_2, PAH, soot
PAH formation model of Richter et al. (Ref. 4)[b]	1999, 2002	PAH

[a] Data available online at http://www.me.berkeley.edu/gri_mech. [b] See also Richter, H., personal communication, 2002.

seen that there is a rather large disagreement with the more recent and presumably more accurate determinations of Davis and Law.[78] The difference between predicted and experimental values is as much as 10 cm/s. This is particularly the case with rich mixtures. Clearly, there is a problem. Although the overall discrepancy might not appear to be large in an absolute sense, the difference is a suggestion that there is a problem with the kinetic model and (or perhaps) the experimental measurements. However, it should be taken into account that to some degree this disagreement reflects the continuous refinement of experimental measurements of heptane burning velocity and continuous refinement of kinetic data.

D. Hierarchical Structure of Kinetic Models of Hydrocarbon Combustion

Because of the hierarchical structure of kinetic models of hydrocarbon combustion, kinetic models for oxidation of larger hydrocabons include models of oxidation of smaller hydrocarbons as submodels. It is natural to assume that kinetics of C_1-C_2 hydrocarbons is well presented by the Grimech 3.0 mechanism because this database was tested against numerous experimental results.* As a first step of model development, we consider the Grimech-3.0 mechanism as the main C_1-C_2 reaction subset of the heptane combustion kinetic model.

There exist alternative kinetic databases for C_1-C_2 hydrocarbon combustion, for example, model.[82] This was developed by Hughes et al.[82] and validated through comparisons with various experimental data on hydrogen, carbon monoxide, methane, and ethane combustion. The principal difference between the databases*[,82] is that the set of rate constants from the Grimech 3.0 model is based on an optimization procedure that compared simulation and experimental data for different reaction systems, whereas the model[82] is largely based on a set of recommended kinetic data.[83]

In this work we will consider the sensitivity of global property—the flame velocity, to the reactions in the kinetic model. Of particular interest will be the modeling of freely propagating heptane flame and the dependence of burning velocity on the equivalence ratio, for which disagreement of modeling results with recent experimental measurements is observed. We will conclude with an analysis of PAH formation in heptane flames. Specific target will be the influence of product distribution of heptyl radical decomposition on PAH production. We will analyze the reaction pathways leading to the formation of aromatic compounds.

III. Kinetic Model of High-Temperature Heptane Combustion

The first step in this project was to develop reaction pathways for the high-temperature degradation of heptane to C_1-C_4 species. This will then serve as inputs to the Grimech-3.0 kinetic model combined with well-tested kinetic models representing combustion of C_3-C_4 hydrocarbons. The construction of heptane kinetic models includes the following steps: 1) determination of decomposition rates of heptane; 2) consideration of heptyl radical formation through hydrogen atom abstraction by radicals; 3) determination of decomposition and isomerization reaction rates of heptyl radicals; 4) determination of rates of hydrogen atom abstraction from olefins formed during heptyl radical decomposition; 5) analysis of decomposition of olefins and olefinic radicals (C_6, C_5 and C_4); 6) assembling of submodel for C3-C4 species based on the models of Marinov et al.,[1] Laskin et al.,[2] Curran et al.,[13] and Richter (personal communication, 2002); and 7) inclusion of Grimech 3.0 as submodel presenting C_1-C_2 species reactions. Kinetic models used in this work are presented in Table 2. Heptane kinetic models analyzed are the kinetic model of Curran et al.,[13] Seiser et al. model,[14] Lidstedt et al. model,[15] and model of Bakali et al.[19] Details of the model development are presented next.

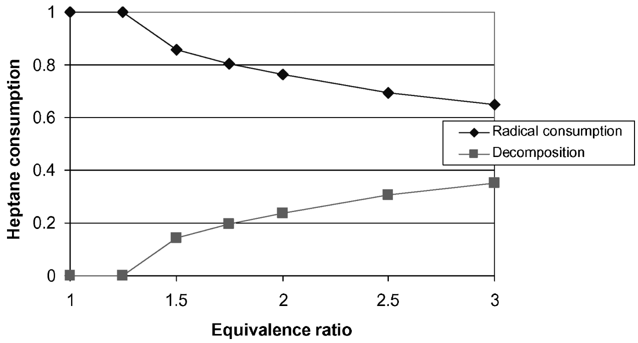

Fig. 2 Contributions of decomposition reactions and radical reactions to heptane consumption (jet stirred reactor, 1650 K, 0.1 MPa, residence time 0.0057 s).

A. Decomposition Rates of n-Heptane

Bakali et al.[19] indicated that decomposition reactions of n-heptane affect the production of benzene, allene, and propyne. They found that exclusion of decomposition channels involving C_2H_5 and 1-C_5H_{11} products leads to changes in the maximum concentrations of benzene and allene in flame zone by 20%. Similar conclusions concerning the effects of the decomposition reactions of heptane were made by Lindstedt and Maurice.[15] It was necessary to include both pyrolysis and radical attack reactions in order to accurately predict intermediate species profiles. Furthermore, the distribution of intermediate species is highly sensitive to the rates of pyrolysis steps. Our calculations of rich heptane combustion indicate that with increase of equivalence ratio contribution of heptane decomposition reactions to overall heptane consumption increases. Figure 2 contains dependencies of contributions of decomposition and radical abstraction reactions to heptane consumption on equivalence ratio.

---

*Data available online at http://www.me.berkeley.edu/gri_mech.

Table 3 Rate constants of heptane decomposition reactions (mol, s, cm, K)

Reaction	log A	n	E/R
$nC_7H_{16} = C_2H_5 + C_5H_{11}$			
$P = 0.1$ MPa	130.877	−32.851	77,855
$P = 1$ MPa	106.605	−25.716	71,273
K_{inf}	25.935	−2.6401	44,273
$nC_7H_{16} = C_6H_{13} + CH_3$			
$P = 0.1$ MPa	132.618	−33.37	79,642
$P = 1$ MPa	108.604	−26.284	73,312
K_{inf}	24.629	−2.2489	45,796
$nC_7H_{16} = nC_3H_7 + nC_4H_9$			
$P = 0.1$ MPa	129.502	−32.451	77,142
$P = 1$ MPa	105.229	−25.322	70,525
K_{inf}	25.885	−2.623	44,443

Table 4 High-pressure rate expressions for the decomposition of heptyl radicals (mol, s, cm, K)

Reactions	log A	n	E/R
C_7H_{15}-1 $= C_2H_4 + nC_5H_{11}$	11.07	0.614	13,358
C_7H_{15}-2 $= C_3H_6 + nC_4H_9$	11.94	0.431	13,702
C_7H_{15}-3 $=$ 1-$C_4H_8 + nC_3H_7$	11.91	0.434	13,674
C_7H_{15}-3 $= CH_3 +$ 1-C_6H_{12}	11.94	0.44	14,748
C_7H_{15}-4 $=$ 1-$C_5H_{10} + C_2H_5$	11.35	0.68	13,397
C_7H_{15}-2 $= C_7H_{15}$-1	2.721	2.429	8,599.3
C_7H_{15}-3 $= C_7H_{15}$-1	3.647	2.362	8,862.6
C_7H_{15}-4 $= C_7H_{15}$-1	5.805	1.961	12,509.7
C_7H_{15}-2 $= C_7H_{15}$-3	5.291	2.117	10,854.8
C_7H_{15}-1 $= C_7H_{15}$-2	3.473	2.205	7,185.3
C_7H_{15}-1 $= C_7H_{15}$-3	4.26	2.211	7,504.9
C_7H_{15}-1 $= C_7H_{15}$-4	6.592	1.734	11,136.3
C_7H_{15}-3 $= C_7H_{15}$-2	5.438	2.042	10,841.2

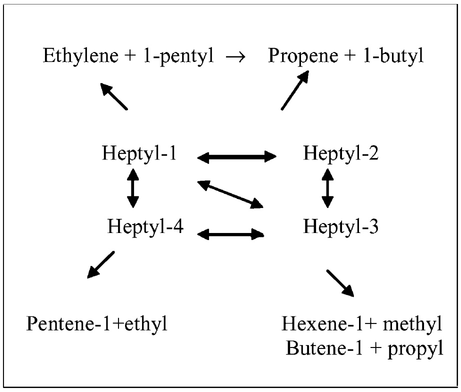

Fig. 3 Reaction pathways of decomposition of heptyl radicals.

It can be seen that at equivalence ratio of 3 heptane consumption in decomposition reactions constitutes approximately 35% of overall consumption rate.

Table 3 contains results of calculations for C-C bond split in heptane. There are three types of C-C bonds in heptane. They are

$$C_7H_{16} = CH_3 + 1\text{-}C_6H_{13}$$

$$C_7H_{16} = C_2H_5 + 1\text{-}C_5H_{11}$$

$$C_7H_{16} = C_3H_7 + 1\text{-}C_4H_9$$

For calculations "Chemrate" program, which has been recently developed to determine energy transfer effects in unimolecular decompositions,[84] was used. The calculations demonstrate that the three reactions all have pressure dependence even at 1 MPa pressure. These results are based on single-pulse shock-tube studies on the decomposition of related hydrocarbons at 1100 K and analogous data for combination of alkyl radicals at room temperatures.

B. Hydrogen Atom Abstraction

Analysis of reaction pathways for heptane consumption shows that the main mechanism for heptane consumption in the flame zone involves the formation of heptyl radicals through hydrogen atom abstraction reactions with H and OH radicals for lean and near-stoichiometric mixtures. Increase of equivalence ratio leads to increasing contributions from heptane decomposition reactions. Recently, Westbrook et al.[66] summarized data for H-atom abstraction from primary, secondary, and tertiary sites in hydrocarbons by different radicals. Rates of hydrogen atom abstraction from heptane by radicals were assumed in accord with the data of this work.

C. Heptyl Radical Isomerization and Decomposition

Decomposition of heptyl radicals in flame leads to a variety of products. The general mechanism is outlined in Fig. 3. 1-C_7H_{15} radical decomposes with formation of C_2H_4 and 1-C_5H_{11}, mostly. 2-C_7H_{15} radical forms 1-C_4H_9 and C_3H_6 species. 3-C_7H_{15} radical has two decomposition channels: 1-C_4H_8 + nC_3H_7 and 1-C_6H_{12} + CH_3. The main products of 4-C_7H_{15} radical decomposition are C_2H_5 and 1-C_5H_{10} species. The essential differences in the kinetic models[13,15,19] are the different reaction rates assigned to heptane reactions with radicals and decomposition reactions of heptyl radicals. Roughly, the different rates of heptane with radicals used in kinetic models lead to formation of different distributions of heptyl radicals in the flame zone. Different description of isomerization and decomposition reactions of heptyl radicals increases the differences in the concentrations of heptyl radicals and the products of its decomposition during heptane consumption. The rate constants assigned for these processes will dictate the branching ratio for the formation of the olefins that can be formed. The nature of the distribution of products can obviously have a very strong effect on the subsequent decomposition process and may have impact on the initiation of soot formation.

We have recently obtained the following high pressure rate expressions for the relevant processes (Table 4). These data represent the first complete set of experimentally based rate expressions for these processes. They are important because they lead to a specific distribution of the smaller compounds that are the inputs to the other modules in the database. Furthermore the heptyl radical decomposition processes are competitive with their oxidation reactions (heptyl + O_2). The consequence is that at the lowest temperatures the oxidation process will predominate and the decomposition processes will not be important. At the highest temperatures decomposition will become the sole reaction and the distribution of products will be of key importance. This leads to possibility of lumping of decomposition and isomerization reactions of heptyl radicals and presentation of these reactions as the lumped hydrogen atom abstraction reactions for heptane with corresponding branching ratios. At the intermediate temperatures the differences between rate constants for oxidation and decomposition can play a key role in the subsequent behavior of the system. We estimate that this intermediate region ranges from 800 to 1000 K for a stoichiometric mixture. This is not an important temperature range for the present application. Thus the branching ratios are sufficient for most applications. Table 5 summarizes the calculated branching ratios.

D. Olefin Kinetics

The products of heptane and heptyl radical decomposition include olefins (1-C_6H_{12}, 1-C_5H_{10} and 1-C_4H_8) and olefinic radicals. Previous kinetic models of heptane combustion treated the formation of olefinic radicals from olefins in terms of lumped species (C_4H_7, C_5H_9, C_6H_{11}). We include reactions of hydrogen atom abstraction from olefins leading to the formation of the following radicals: 1-C_4H_7-3, 1-C_4H_7-4, 1-C_5H_9-3, 1-C_5H_9-4, 1-C_5H_9-5, 1-C_6H_{11}-3, 1-C_6H_{11}-4, 1-C_6H_{11}-5, and 1-C_6H_{11}-6. Rate constants for these processes are based on recent results of Sumathi et al.[85] For H-atom abstraction from olefins by radicals different from the hydrogen atom, the overall rate constants suggested by Curran et al.[13] with branching coefficients for abstraction by hydrogen atom[85] are used as a first approximation. Kinetic data for decomposition of olefins and

Table 5 Branching ratios for decomposition of heptyl radical[a]

Initial radical	Decomposition reactions	log *A*	n	E/R, K
$C_7H_{15}\text{-}1$	$C_7H_{15}\text{-}1 => C_2H_4 + nC_5H_{11}$	−1.09	−0.345	1824
	$C_7H_{15} - 2 => C_3H_6 + nC_4H_9$	9.82	3.195	1988
	$C_7H_{15} - 3 => 1\text{-}C_4H_8 + nC_3H_7$	9.05	2.83	2183
	$C_7H_{15}\text{-}3 => CH_3 + 1\text{-}C_6H_{12}$	5.62	1.869	2069
	$C_7H_{15} - 4 => 1\text{-}C_5H_{10} + C_2H_5$	−3.66	0.935	291
$C_7H_{15}\text{-}2$	$C_7H_{15}\text{-}1 => C_2H_4 + nC_5H_{11}$	3.128	1.384	1274
	$C_7H_{15} - 2 => C_3H_6 + nC_4H_9$	0.364	0.121	399
	$C_7H_{15} - 3 => 1\text{-}C_4H_8 + nC_3H_7$	0.277	0.375	−392.8
	$C_7H_{15}\text{-}3 => CH_3 + 1\text{-}C_6H_{12}$	−2.93	−0.523	−452
	$C_7H_{15} - 4 => 1\text{-}C_5H_{10} + C_2H_5$	1.458	1.045	69.7
$C_7H_{15}\text{-}3$	$C_7H_{15}\text{-}1 => C_2H_4 + nC_5H_{11}$	4.36	1.646	1838
	$C_7H_{15} - 2 => C_3H_6 + nC_4H_9$	1.33	0.724	−287.2
	$C_7H_{15} - 3 => 1\text{-}C_4H_8 + nC_3H_7$	1.2	0.415	482.1
	$C_7H_{15}\text{-}3 => CH_3 + 1\text{-}C_6H_{12}$	−2.875	−0.733	187.8
	$C_7H_{15} - 4 => 1\text{-}C_5H_{10} + C_2H_5$	2.98	1.375	785.6
$C_7H_{15}\text{-}4$	$C_7H_{15}\text{-}1 => C_2H_4 + nC_5H_{11}$	−7.86	−1.91	153.5
	$C_7H_{15} - 2 => C_3H_6 + nC_4H_9$	2.56	1.46	493.5
	$C_7H_{15} - 3 => 1\text{-}C_4H_8 + nC_3H_7$	3.28	1.52	1154
	$C_7H_{15}\text{-}3 => CH_3 + 1\text{-}C_6H_{12}$	0.1148	0.632	1100.4
	$C_7H_{15} - 4 => 1\text{-}C_5H_{10} + C_2H_5$	0.124	0.0413	38.1

[a] Expressions are in the form of $A*(1/T)^n\exp(-E/RT)$.

olefinic radicals were in accord with the results of Tsang.[8] The incorporation of this block of reactions into the model provides a more accurate kinetic description of decomposition/oxidation pathways of olefins, which are important for PAH and soot formation modeling.

E. C1-C4 Reaction Block

The submodel of C_3-C_4 species reactions was mainly assembled from the models of Laskin et al.,[2] Marinov et al.,[1] Curran et al.,[13] and H. Richter (personal communication, 2002). The model includes the optimized C_1-C_3 kinetics database that was calibrated to fit the burning velocity dependencies of C_1-C_3 hydrocarbons on the equivalence ratio and temperature dependence of ignition delay.[86] This represents an extended version of the Grimech 3.0 mechanism* and constitutes the basic set of reactions of C_1-C_3 species in the heptane kinetic model. More detailed discussion concerning the modification of rates for some reactions of Grimech-3.0 model is given in the section on laminar premixed flame modeling.

F. Kinetics of PAH Growing Process

For modeling of PAH growing process, the kinetic submodel was assembled using the kinetic databases of Marinov et al.,[1] Appel et al.,[3] and Richter et al.[4] (also Richter, H., personal communication, 2002). Additional reactions and updates of rate constants were included from several recent sources.[5–7] The model was extended by analogy to include reactions of PAH formation up to ovalene. Additionally, calculations were conducted with the use of PAH formation database of Marinov et al.[1] and Appel et al.[3] as published for comparison purposes.

The overall kinetic database includes 1745 reactions with 347 species. Thermochemical data were from standard sources.[1,3,4,6,13,15,*] (also Richter, H., personal communication, 2002). Where data were unavailable, data were estimated with the use of National Institute of Standards and Technology Structures and Properties program[87] and through the use of the group additivity procedure.[88,89] The Chemkin-2 package was used for the simulation work.[90]

IV. Comparison with Experimental Data

Different parts of the database have been tested in the original investigations. For example, the optimized C3 mechanism,[86] which is based on Grimech model,* was tested against numerous experimental data for C_1-C_3 hydrocarbon systems. Marinov et al.[1] tested their model of PAH formation against experimental data on flame structure for propane and butane flames. Comparison of modeling results on heptane combustion with experimental data was conducted for the following set of experimental data: dependence of burning velocity of heptane/air on equivalence ratio (next section), temperature dependence of ignition delay of heptane/oxygen mixtures behind shock wave, and OH time history during ignition behind shock wave.

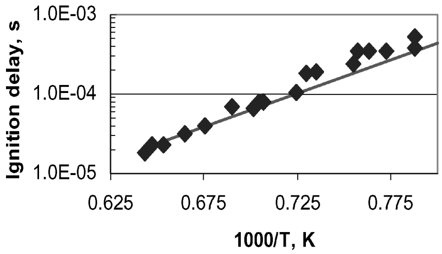

Fig. 4 Temperature dependence of heptane ignition delay behind shock wave (2.5% heptane, 27.5% O_2, 70% Ar): ■, experimental data,[91] 0.19–0.26 MPa; ——, this work, 0.23 atm.

Vermeer et al.[91] studied high-temperature ignition of heptane/oxygen mixtures behind reflected shock waves for pressure range 1–4 atm and temperatures 1200–1700 K. Results are summarized in Fig. 4 and are in a good agreement with the calculated temperature dependence of the ignition delay. The calculated ignition delay was taken as the time to achieve maximum concentration of the CH radical. The simulations show that heptane is decomposed before ignition. Thus ignition occurs in the presence of significant amount of the decomposition products (C_2H_4, C_3H_6, $1\text{-}C_4H_8$, $1\text{-}C_6H_{12}$, $1\text{-}C_5H_{10}$, and associated radicals). The ignition process can be characterized in terms of two-stage process, where the heptane decomposition is the first stage and the second stage corresponds to ignition of decomposition products of heptane.

Horning et al.[92] have studied ignition of n-heptane behind reflected shock waves over the temperature range of 1300–1700 K and for 0.1–0.6 MPa pressure range. Figure 5 contains comparisons of modeling results of temperature dependencies of ignition delays for lean, stoichiometric and rich heptane/oxygen mixtures at 1 bar. The ignition time was defined as before.[92] It can be seen that calculated ignition delays are about 20–30% shorter than experimentally determined ones for all three mixture compositions depending on the initial temperature.

Davidson et al.[93] measured OH radical concentration evolution behind reflected shock waves in the oxidation of n-heptane. Initial conditions of these measurements were 1360–1780 K and 0.202–0.38 MPa. Experiments were performed for equivalence ratios 0.8–1.2 and concentration of fuel in mixture 200–300 ppm. Figure 6

---

*Data available online at http://www.me.berkeley.edu/gri_mech.

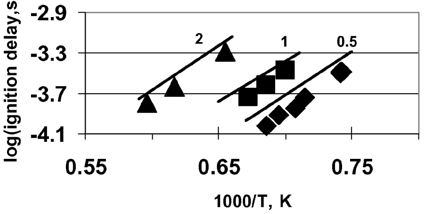

Fig. 5 Temperature dependence of heptane ignition delay for different equivalence ratios (0.5, 1, 2; 0.4% heptane), pressure 0.1 MPa: ▲, ■, experimental data[92]; ——, this work.

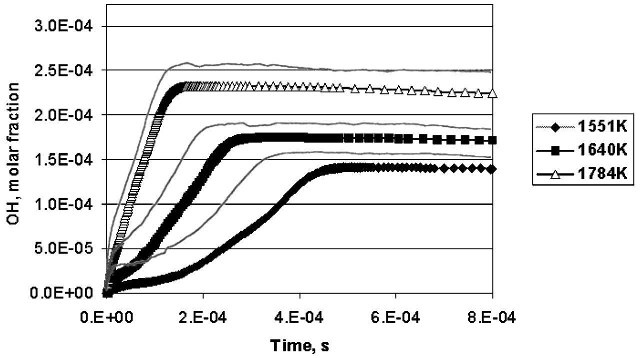

Fig. 6 OH concentration for different temperatures: ——, experimental data[93]; ◆, ■, △, this work [300 ppm C_7H_{16}, heptane/O2/Ar, equivalence ratio 1; 1551 K (0.214 MPa); 1640 K (0.204 MPa), 1784 K (0.212 MPa)].

Table 6 Normalized sensitivity coefficients for heptane/air flame (dependence on equivalence ratio)

Reaction/equivalence ratio	0.8	1	1.4
$H + O_2 = OH + O$	0.205	0.23	0.703
$CH_3 + H + M = CH_4 + M$	−0.0198	−0.0249	−0.262
$HCO + M = H + CO + M$	0.0435	0.042	0.0846
$OH + CO = CO_2 + H$	0.143	0.0857	0.032
$H + O_2 + M = HO_2 + M$	−0.0838	−0.040	−0.019
$H + aC_3H_5 + M = C_3H_6 + M$	−0.053	−0.043	−0.11
$H + C_2H_4 + M = C_2H_5 + M$	0.00971	0.00965	0.03

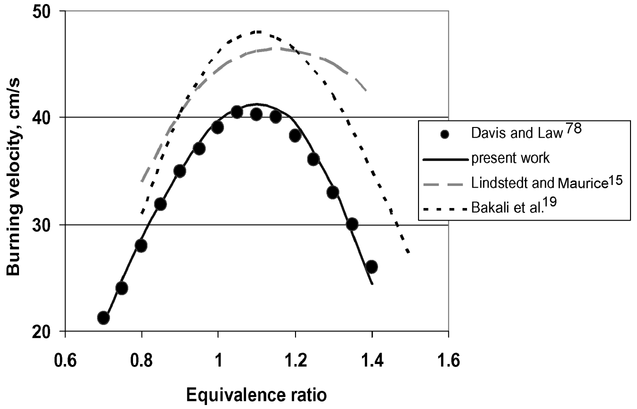

Fig. 7 Dependence of heptane burning velocity on equivalence ratio; ●, experimental data[78]; ——, – – –, · · · ·, results of calculations (Refs. 15, 19, and present work).

contains experimental and modeling results for three different temperatures and stoichiometric mixtures. There is reasonable agreement for OH evolutions measured at different temperatures.

V. Burning Velocity of Heptane Combustion

Figure 7 illustrates the dependence of the laminar burning velocity on equivalence ratio and demonstrates that detailed kinetic models[15,19] overpredict burning velocity in comparison with experimental data of Davis and Law.[78] Calculations were also conducted using a combination of Grimech 3.0 with the reduced Seiser et al. model.[14] Reduction of Seiser et al. model involved the exclusion of reactions with hydrocarbon peroxides and hydroperoxy radicals. These reactions are important for low-temperature range and conditions typical for NTC conditions. As before, this combined model substantially overpredicts burning velocity in comparison with the data.[78]

We have also made calculations using a combination of the Grimech-3.0 database* on C_1-C_2 species kinetics with those of Lindstedt and Maurice[15] and Bakali et al.[19] for the larger species. This is similar in spirit with the combined model of Seiser et al.[14] The calculated burning velocities (the range of equivalence ratio was 0.8–1.2) deviated from each other by less than 3–5%. This demonstrates that the main reactions contributing to the burning velocity correspond to reactions in the C_1-C_2 system, with the inclusion of some reactions of the C_3 species. As was the case with the combined Seiser et al. database,[14] the burning velocity was overpredicted when compared with the latest experiments.

A. Sensitivity Analysis

Figures 8–10 contain results of calculations on the sensitivity of flame velocity to the reactions in the combined reduced model of Seiser et al.[14] with Grimech 3.0 (Ref. 74), Bakali et al. model,[19] and Lindstedt and Maurice model.[15] In general, the models demonstrate that reactions controlling the heat-release kinetics in heptane flames are similar to reactions of C_1-C_4 hydrocarbon flames.[103] Nevertheless, they have different patterns of sensitivity coefficients. For example the results of Lindstedt and Maurice[15] show that the flame velocity is more sensitive to the rate constant of HCO radical decomposition than those of the reactions $HCO + H = H_2 + CO$ and $CH_3 + CH_3 = C_2H_5 + H$. Calculations from the database in the work of Bakali et al.[19] demonstrate that the flame velocity is equally dependent on the rate constants for the three reactions.

Sensitivity calculations reveal that the main reactions determining burning velocity are the reactions $H + O_2 = H + OH$, $CO + OH = CO_2 + O$, $H + O_2 + M = HO_2 + M$, $HCO + M = H + CO + M$, $H + HCO = CO + H_2$, $CH_3 + CH_3 = C_2H_5 + H$, $C_2H_5 = C_2H_4 + H$, and $H + aC_3H_5 = C_3H_6$. In all cases, the influence of reactions involving the C_5-C_7 species on burning velocity is small or less than 2–4% of the sensitivity level for the chain branching reaction $H + O_2 = OH + O$. Within these small limits, the following reactions involving heptane make the most contributions: $C_7H_{16} + OH = 2\text{-}C_7H_{15} + H_2O$, $C_7H_{16} + H = C_7H_{15} + H_2$, $C_7H_{16} + OH = 3\text{-}C_7H_{15} + H_2O$, and heptyl radical decomposition $1\text{-}C_7H_{15} = aC_5H_{11} + C_2H_4$, $2\text{-}C_7H_{15} = aC_4H_9 + C_3H_6$, $1\text{-}C_7H_{15} = 2\text{-}C_7H_{15}$. OH attack is particularly important for lean and stoichiometric flames. The model of Seiser et al.[14] shows that the most important reactions of C7 species with respect to the flame velocity correspond to the reactions of heptane with H and OH radicals. On the other hand, the models of Lindstedt and Maurice[15] and Bakali et al.[19] demonstrate some sensitivity to the rate constant for the decomposition of heptyl radical $1\text{-}C_7H_{15} = 1\text{-}C_5H_{11} + C_2H_4$ and $2\text{-}C_7H_{15} = C_3H_6 + p\text{-}C_4H_9$.

Table 6 contains calculated sensitivity coefficients of the main reactions for lean, stoichiometric, and rich mixtures. In all cases the flame velocity was most sensitive to the reactions of C1-C2 hydrocarbon species. With increasing equivalence ratio, the sensitivity of burning velocity to the rate constant of $CH_3 + H + M = CH_4 + M$ reaction increases substantially. Burning velocity of lean mixture compositions is more sensitive to the reactions $H + O_2 + M = HO_2 + M$ and $CO + OH = CO_2 + H$. Increase of equivalence ratio decreases sensitivity to these reactions. The sensitivity to rate constants of C3-C4 species reactions remains approximately at the same level with the change of equivalence ratio. It is of interest that most of reactions with positive sensitivities correspond to reactions, which produce hydrogen atom. Negative sensitivity coefficients correspond to reactions mainly consuming hydrogen atom.

---

*Data available online at http://www.me.berkeley.edu/gri_mech.

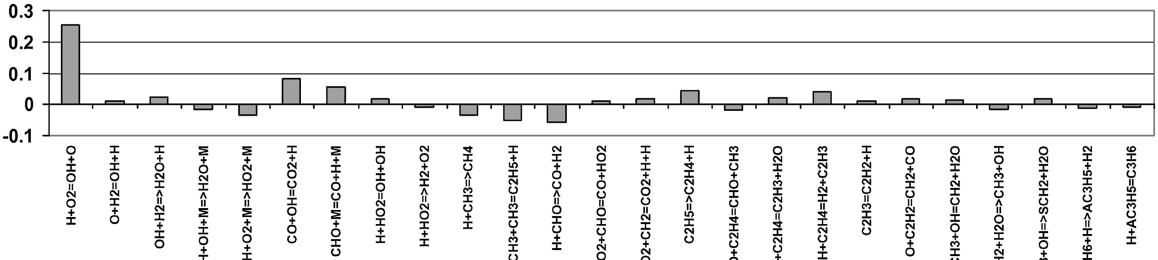

Fig. 8 Sensitivity coefficients for heptane/air flame, kinetic model of Bakali et al.[19]

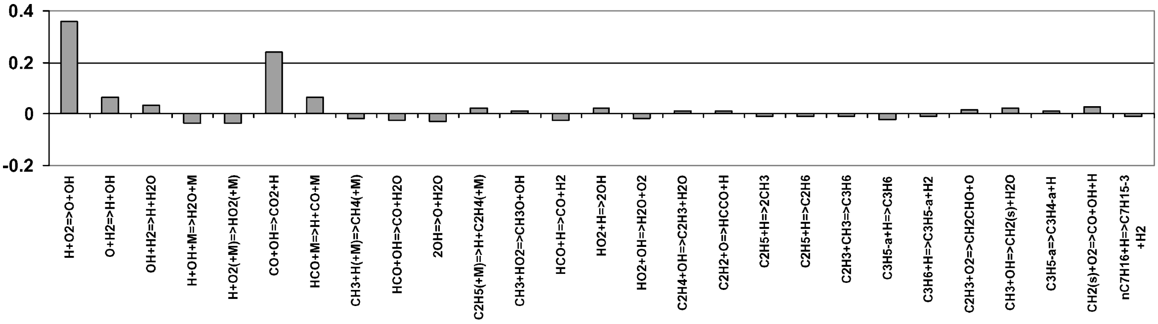

Fig. 9 Sensitivity coefficients for heptane/air flame, Grimech 3.0 and reduced kinetic model of Seiser et al.[14]

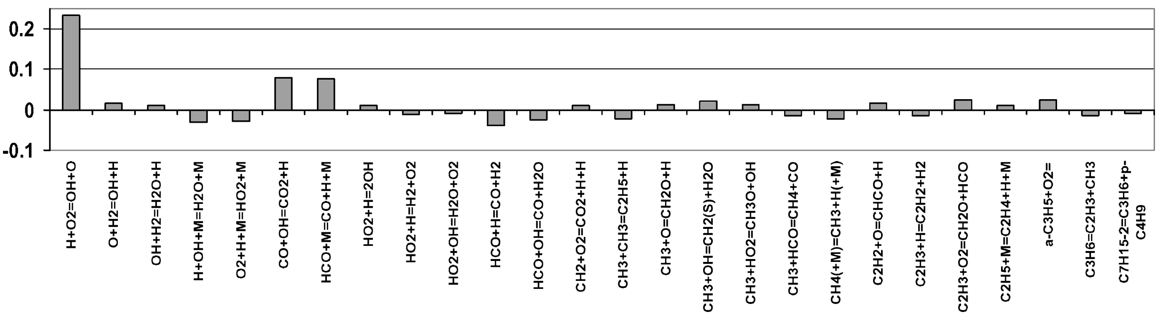

Fig. 10 Sensitivity coefficients for heptane/air flame, kinetic model of Lindstedt and Maurice.[15]

B. Modification of Grimech-3.0 Model

The simulation results show that modification of the kinetic model for the reactions involving C_1-C_3 species is required if the agreement is to be achieved between simulation and experimental results on the relation between burning velocity and equivalence ratio. Sensitivity analysis does not reveal reactions with the relatively large sensitivity coefficients from C_5-C_7 reaction sub-system. The main reactions influencing burning velocity are the reactions of C_1-C_3 hydrocarbon species and they are general part of the Grimech-3.0 model. Unfortunately this means that some aspects of the well tested Grimech-3.0* database dealing with the C_1-C_2 reaction subset must be adjusted.

Recently Qin et al.[86] developed a kinetic database for propane combustion using Grimech 3.0 mechanism as a basis for the C_1-C_2 reaction subset. It was found that the first version of the mechanism also substantially overpredicts the burning velocity of propane. The authors[86] concluded that for fitting experimental data on burning velocities and ignition delay modifications of the rate constants for the base model—methane combustion—is required. A reasonable match to experimental data on burning velocity and ignition delays for C_1-C_3 hydrocarbons was obtained by reoptimizing of nine rate constants of the Grimech 3.0 kinetic model.

Table 7 contains the set of reactions whose rate constants were adjusted to fit calculations and experiments for propane combustion in the original publication.[86] Also included are the set of reactions modified in this work in such a manner as to provide agreement with the experimental data on burning velocity of Davis and Law.[78] This set is based on sensitivity analysis, effects arising from variations of rate constant, and analysis of available data on rate constant for various processes. It includes four reactions from Grimech-3.0 kinetic model compared to nine reactions suggested by Qin et al.[86] Two of these reactions correspond to the set of reactions of Qin et al.[86] Other suggested reactions correspond to C_3 reaction subsystem. Most of these reactions involve the formation and consumption of allyl radical.

Propene is an important product from heptyl radical decomposition. It is also formed during the decomposition of olefins and olefinyl radicals. Allyl radicals are very stable and can therefore inhibit chain processes by combination with radicals. They are also an important precursor for aromatic formation. This is readily demonstrated from sensitivity calculations. Increasing the reaction rates of channels with allyl radical formation leads to burning velocity decreases, as a result of inhibition sequence of reactions involving allyl radical:

$$C_3H_6 + H\ (O, OH) = aC_3H_5 + H_2\ (OH, H_2O)$$

$$aC_3H_5 + H + M = C_3H_6 + M$$

Recombination of allyl radical with hydrogen leads to propene formation and permits through hydrogen atom attack some cycling and catalytical recombination of H atom, thus decreasing burning velocity.

---

*Data available online at http://www.me.berkeley.edu/gri_mech.

Table 7 Set of reactions used to fit experimental data

Set of reactions used for optimization by Qin et al.[86]	Set of reactions determined in this work
$C_2H_4 + OH = C_2H_3 + H_2O$ (*)[a]	——
$C_2H_4 + O = H + CH_2CHO$ (*)	——
$C_2H_4 + O = CH_3 + HCO$ (*)	——
$H + C_2H_4 + M = C_2H_5 + M$ (*)	$H + C_2H_4 + M = C_2H_5 + M$ (*)
$C_2H_3 + O_2 = O + CH_2CHO$ (*)	$C_2H_3 + O_2 =>$ (*)
$C_2H_3 + H = H_2 + C_2H_2$ (*)	——
$CH_3 + HO_2 = CH_3O + OH$ (*)	——
$HO_2 + H = OH + OH$ (*)	——
$HO_2 + H = H_2 + O_2$ (*)	——
——	$H + CH_3 + M = CH_4 + M$ (*)
——	$HCO + M = H + CO + M$ (*)
$C_3H_6 + H = aC_3H_5 + H_2$	$C_3H_6 + H = aC_3H_5 + H2$
$C_3H_6 + OH = aC_3H_5 + H_2O$	$C_3H_6 + OH = aC_3H_5 + H_2O$
$C_3H_6 + H = C_2H_4 + CH_3$	——-
$aC_3H_5 + H + M = C_3H_6 + M$	$aC_3H_5 + H + M = C_3H_6 + M$
——	$aC_3H_5 + O =>$
——	$C_3H_6 + O = aC_3H_5 + OH$
——	$aC_3H_4 + H + M = aC_3H_5 + M$
——	$CH_3 + C_2H_2 + M = a\text{-}C_3H_5 + M$

[a](*) denotes reactions considered in the Grimech-3.0 model. (Data available online at http://www.me.berkeley.edu/gri_mech.)

As a first approach to developing of heptane combustion model, we follow suggestions of Qin et al.[86] It is of interest to indicate that optimization of the C_1-C_3 model[86] was conducted without taking into account constraints determined by branching ratios, for example, data for process $H + HO_2 =>$ products were modified without taking into account that there exist certain branching ratio for the channels of this reaction, which is important for modeling of self-ignition processes and ignition in the intermediate temperature range. Also, data for reactions of formation aC_3H_5 in the radical reactions with C_3H_6 were modified without corresponding corrections for other channels of these processes. Thus, future additional justification of these modifications will be needed.

C. Effect of $C_2H_3 + O_2$ Reaction

The reaction of vinyl and O_2 is another high sensitivity reaction. Reaction of vinyl radical with oxygen was analyzed in several works.[94–98] It is one of the main reactions that determine the level of conversion of C2 species into those with one carbon atom. The following channels were considered in the kinetic model for this multichannel process:

a) $$C_2H_3 + O_2 = C_2H_2 + HO_2$$

b) $$C_2H_3 + O_2 = HCO + CH_2O$$

c) $$C_2H_3 + O_2 = O + CH_2CHO$$

Calculations demonstrate that burning velocity is sensitive to the channel c) with $O + CH_2CHO$ products, which is the chain branching process. It was noted that channel b) leading to the formation of $CH_2O + HCO$ is most important at low temperatures. As the temperature is increased, channel a) with $C_2H_2 + HO_2$ formation becomes important.[82,83,94] It was indicated that in order to have reasonable prediction of ignition delays in ethane/O_2/Ar mixtures it is necessary to have the $HO_2 + C_2H_2$ channel despite the lack of experimental evidence for it.[83,94] The reaction of C_2H_3 with O_2 has to be assumed to have the products HO_2 and C_2H_2 at high temperature, in contrast to low-temperature measurements where the products are HCO and CH_2O. Otherwise no reasonable results for ignition delay times and burning velocities are possible.[82,83]

Mebel et al.[96] have analyzed this reaction theoretically and computed rate constants for all three channels. They concluded that in the temperature range 500–900 K the channel a) forming $CHO + CH_2O$ dominates. With increasing temperature ($T > 900$ K) the chain branching c) process becomes more important. It is only at the highest temperatures ($T > 2500$ K) that the channel yielding $C_2H_2 + HO_2$ products begin to make contributions.[96] These rate constants were used in Grimech 3.0 model. Marinov et al.[1] used different ratio of rate constants, based on the work of Westmoreland[95] and calculations of Melius for reaction b) (Marinov, N. M., personal communication, 2001). The rate constant for chain branching channel c) obtained by Wesmoreland[95] was increased by Marinov et al.[1] (see also Marinov, N. M., personal communication, 2001) because of the necessity to match experimental data for acetylene concentrations in rich flames. Recently Carriere et al.[98] concluded that the channel with $CH_2CHO + O$ products does not make contribution until ~2300 K. Our results confirm the claim that the rate constant assigned in Grimech-3.0 model for this channel is too high if agreement between simulations and experimental data on burning velocity is to be achieved.

The overall rate constant was measured by Fahr and Laufer[99] and Knyazev and Slagle.[100] Based on these measurements, Baulch et al.[83] recommended temperature-independent value 5.42×10^{12} for overall rate constant. This value was used for channel a) in the model[82] to represent the reaction $C_2H_3 + O2$. Note that in the Grimech 2.11 model reaction of vinyl radical with oxygen was represented by channel b) only. Qin et al.[86] decreased the rate constant for chain branching channel by a factor of 0.4. The decreased rate constant coincides with the data used by Marinov et al.[1] at temperature approximately 1380 K, but the temperature dependencies are different.

VI. Influence of Product Distribution of Heptyl Radical Decomposition on PAH Formation

The values of the rate constants assigned to the formation, isomerization, and decomposition of heptyl radicals determine the level and distribution of the PAHs. The main stable products from heptyl radicals are CH_4, C_2H_4, C_3H_6, 1,3-C_4H_6, 1-C_5H_{10}, and 1-C_6H_{12}. Calculated distribution of hydrocarbon products from heptane oxidative decomposition at the maximum of C_3H_6 and 1,3-C_4H_6 concentrations is CH_4:C_2H_2:C_2H_4:C_2H_6:C_3H_6:1,3-C_4H_6 = 2.4:1.3:12:1.2:2.6:1 for an equivalence ratio 2 in a jet stirred reactor. This ratio approximately coincides with the product distribution for stoichiometric mixtures at the position of maximum concentrations of C_3H_6 and 1,3-C_4H_6. Details of PAH growing processes at high temperatures were analyzed through the modeling of combustion process in jet stirred reactor. Calculations of freely propagating heptane flames with kinetic model including PAH formation processes require large times of computer processor. Figure 11 contains dependencies of intermediate products of high-temperature heptane combustion on residence time in a jet stirred reactor. It shows the changes in the branching ratio of heptane products with the residence time during heptane consumption.

Figures 12 contains the results of calculations of PAH yields for the combustion of a variety of hydrocarbons (CH_4, C_2H_6, C_2H_4, C_2H_2, C_3H_8, C_3H_6, C_4H_{10}, 1-C_4H_8, 1,3-C_4H_6, and heptane) at the same equivalence ratio. The lowest production of C_6H_6, $C_{10}H_8$, phenanthrene, and pyrene correspond to methane combustion. The maximum yield corresponds to 1,3-butadiene. In terms of propensity for PAH production, the 1,3-butadiene is followed by propylene

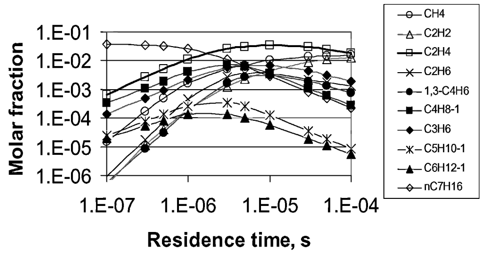

Fig. 11 Dependence of intermediate products of heptane combustion on residence time (equivalence ratio 2, 1650 K, 0.1 MPa).

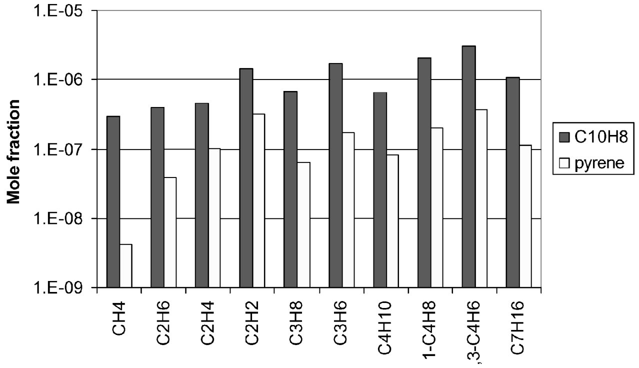

Fig. 12 **Concentrations of naphthalene and pyrene for combustion of different hydrocarbons (equivalence ratio 2; 1650 K, 0.0057 s, 0.1 MPa).**

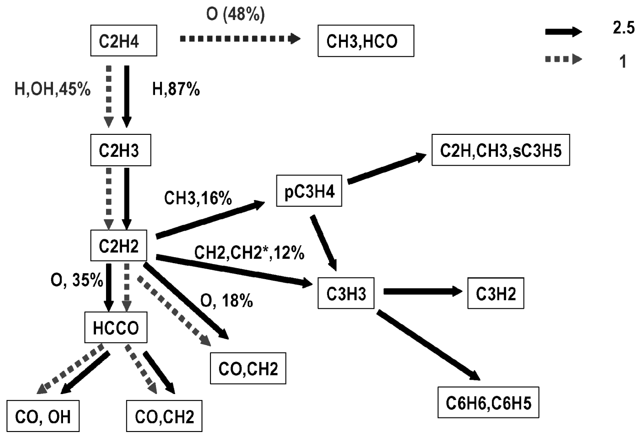

Fig. 13 **Consumption pathways of ethylene (equivalence ratios 1 and 2.5, 1650 K, residence time 0.0057 s, 0.1 MPa).**

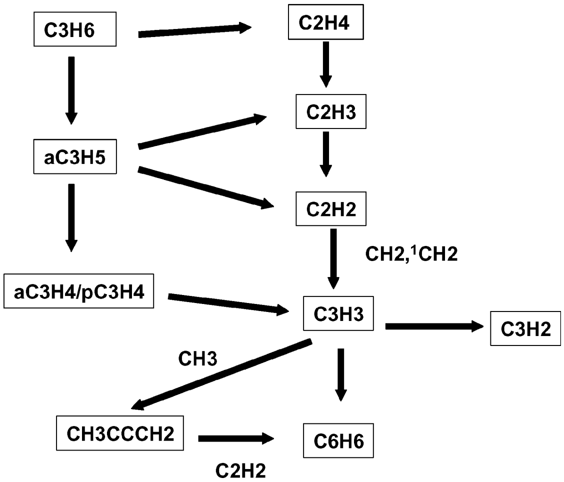

Fig. 14 **Major reaction routes of propargyl radical and benzene formation for propylene combustion (equivalence ratio 2; 1650 K, 0.0057 s, 0.1 MPa).**

and 1-C_4H_8. Heptane is comparable with ethylene in the production of pyrene. Figure 12 demonstrates the increasing of PAH production with the number of carbon atoms in the alkanes. These results correlate with experimental data on critical sooting equivalence ratio for premixed hydrocarbon flames.[101]

Figure 13 contains major reaction pathways of propargyl radical and benzene formation for ethylene combustion. Note that ethylene represents the main product of decomposition of heptyl radicals. Propargyl radicals are formed in the reactions of CH_2 and $^1CH_2$ with acetylene. Hydrogen atom abstraction from pC_3H_4 is a minor channel. Benzene formation is largely a result of reactions of propargyl radical combination. Figure 14 contains reaction pathways of propargyl radical and benzene formation for propylene combustion. Our mechanism highlights the route to propargyl radical formation through allyl radical and successive hydrogen atom abstraction. The reaction pathways of benzene formation in C_3H_6 combustion were discussed by Pope and Miller,[102] and they are in accord with our conclusions. Figure 15 presents reaction pathways of propargyl and benzene formation for combustion of 1,3-butadiene. For 1,3-butadiene the following reaction pathway provides additional contributions to the formation of propargyl radical and benzene: $1,3\text{-}C_4H_6 + H(OH) = CH_2CHCCH_2 + H_2$ (H_2O); $CH_2CHCCH_2 = CH_3CCCH_2$; $CH_3CCCH_2 + H = C_3H_3 + CH_3$; and $CH_3CCCH_2 + C_2H_2 = C_6H_6 + H$. Figure 16 contains simplified reaction pathways of propargyl and benzene formation for combustion of heptane in jet stirred reactor. It demonstrates that formation of ring compounds for heptane combustion represents some combination of reaction pathways of benzene and propargyl radical, formation for ethylene and propylene combustion at analyzed conditions of reaction proceeding. Formation of ethylene, 1-C_4H_8, 1-C_5H_{10}, pC_4H_9, C_3H_6, nC_3H_7, C_2H_5 as the result of decomposition and isomerization reactions of heptyl radicals leads to two major reaction routes in the generation of propargyl radicals and benzene. First route includes formation aC_3H_5 radical, which leads to formation of aC_3H_4/pC_3H_4 and C_2H_3 species. Reactions of aC_3H_4 and pC_3H_4 lead to the formation of C_3H_3. Second pathway incorporates formation of ethylene from C_2H_5 and nC_3H_7 radicals, which leads to propargyl radical through formation of C_2H_3 and C_2H_2.

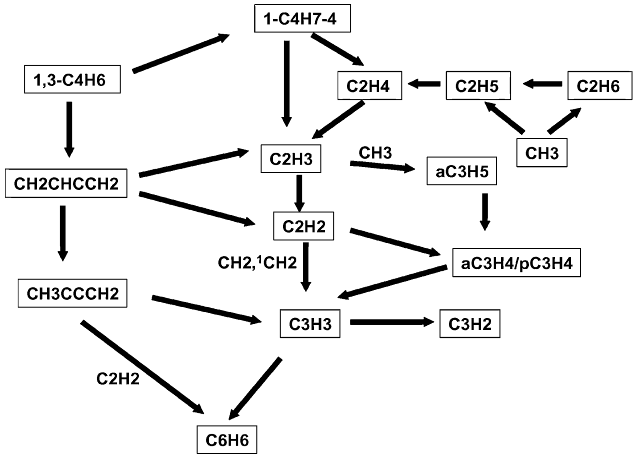

Fig. 15 **Major reaction routes of propargyl radical and benzene formation for 1,3-butadiene combustion (equivalence ratio 2; 1650 K, 0.0057 s, 0.1 MPa).**

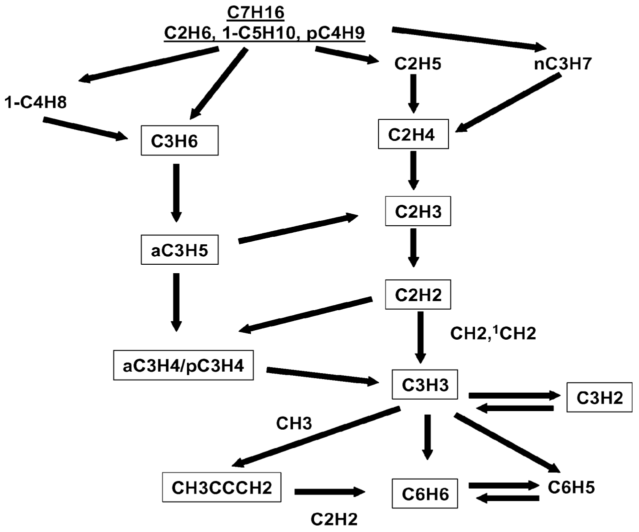

Fig. 16 **Major reaction routes of propargyl radical and benzene formation for heptane combustion (equivalence ratio 2; 1650 K, 0.0057 s, 0.1 MPa).**

VII. Conclusions

We have studied the kinetics of heptane combustion at high temperatures through numerical modeling. A kinetic model of high-temperature heptane combustion was constructed. The model is based on new kinetic data for decomposition of heptane, olefins, heptyl and olefinic radicals. The model includes four major blocks of reactions: C_1-C_2 chemistry, which is based on Grimech-3.0 model[86,*]; block of C_3-C_4 reactions based on the models[1,2] (see also Richter, H., personal communication, 2002); and block of C_4-C_7 reactions, which is based on new results and previous heptane combustion models.[8,13–15,66] A block of reactions of PAH formation was assembled based on the models of Marinov et al.,[1] Richter (personal communication, 2002), and ABF model.[3] The modeling of heptane combustion was concentrated on the simulation of burning velocity dependence on equivalence ratio and temperature dependence of ignition delay at high temperatures. Comparison of modeling results with experimental data on burning velocity of Davis and Law,[78] ignition delay of Vermeer et al.[91] and Horning et al.,[92] and OH kinetics behind shock waves[93] demonstrates reasonable agreement. Rate constants for heptane decomposition were calculated. It was demonstrated that for 0.1 and 1 MPa pressures decomposition of n-heptane proceeds in fall-off region and rate constants are pressure dependent. The reactions determining burning velocity were established through sensitivity analysis. The main reactions determining burning velocity are similar to reactions determining burning velocity of C1-C4 hydrocarbons. Sensitivity of burning velocity to reactions of C5-C7 species is relatively small. Modeling of influence of product distribution of heptyl radical decomposition on PAH formation demonstrates that reaction pathway of formation of first aromatic compounds represents some combination of reaction pathways of benzene and propargyl radical formation in ethylene and propylene combustion.

Acknowledgments

The authors would like to thank F. Dryer, N. Peters, H. Richter, R. Seiser, and C. Vovelle for providing their kinetic models. Financial support from the Strategic Environmental Research and Development Program (Charles Pellerin, manager) is acknowledged.

References

[1] Marinov, N. M., Pitz, W. J., Westbrook, C. K., Vincitore, A. M., Castaldi, M. J., Senkan, S. M., and Melius, C. F., "Aromatic and Polycyclic Aromatic Hydrocarbon Formation in a Laminar Premixed n-Butane Flame," *Combustion and Flame*, Vol. 114, Nos. 1–2, 1998, pp. 192–213.

[2] Laskin, A., Wang, H., and Law, C. K., "Detailed Kinetic Modeling of 1,3-Butadiene Oxidation at High Temperatures," *International Journal Chemical Kinetics*, Vol. 32, No. 10, 2000, pp. 589–614.

[3] Appel, J., Bockhorn, H., and Frenklach, M., "Kinetic Modeling of Soot Formation with Detailed Chemistry and Physics: Laminar Premixed Flames of C2 Hydrocarbons," *Combustion and Flame*, Vol. 121, Nos. 1–2, 2000, pp. 122–136.

[4] Richter, H., Grieco, W. J., and Howard, J. B., "Formation Mechanism of Polycyclic Aromatic Hydrocarbons and Fullerenes in Premixed Benzene Flames," *Combustion and Flame*, Vol. 119, Nos. 1–2, 1999, pp. 1–22.

[5] D'Anna, A., Violi, A., and D'Alessio, "Modeling the Rich Combustion of Aliphatic Hydrocarbons," *Combustion and Flame*, Vol. 121, 2000, pp. 418–429.

[6] Lindstedt, P., Maurice, L., and Meyer, M., "Thermodynamic and Kinetic Issues in the Formation and Oxidation of Aromatic Species," *Faraday Discussions*, No. 119, 2001, pp. 409–432.

[7] Bohm, H., and Jander, H., "PAH Formation in Acetylene-Benzene Pyrolysis," *Physical Chemistry Chemical Physics*, Vol. 1, No. 16, 1999, pp. 3775–3781.

[8] Tsang, W., "Progress in the Development of a Kinetic Data Base for Heptane Combustion," AIAA Paper 2003-0063, Jan. 2003.

[9] Warnatz, J., "Chemistry of High Temperature Combustion of Alkanes up to Octane," *Proceedings of the Combustion Institute*, Vol. 20, 1984, pp. 845–856.

[10] Nehse, M., Warnatz, J., and Chevalier, C., "Kinetic Modeling of the Oxidation of Large Aliphatic Hydrocarbons," *Proceedings of the Combustion Institute*, Vol. 26, 1996, pp. 773–780.

[11] Westbrook, C. K., Warnatz, J., and Pitz, W. J., "A Detailed Chemical Kinetic Reaction Mechanismfor the Oxidation of Iso-Octane and n-Heptane over an Extended Temperature Range and its Application to Analysis of Engine Knock," *Proceedings of the Combustion Institute*, Vol. 22, 1988, pp. 893–901.

[12] Chevalier, C., Pitz, W. J., Warnatz, J., Westbrook, C. K., and Melenk, H., "Hydrocarbon Ignition: Automatic Generation of Reaction Mechanisms and Applications to Modeling of Engine Knock," *Proceedings of the Combustion Institute*, Vol. 24, 1992, pp. 93–101.

[13] Curran, H. J., Gaffuri, P., Pitz, W. J., and Westbrook, C. K., "A Comprehensive Modeling of n-Heptane Oxidation," *Combustion and Flame*, Vol. 114, 1998, pp. 149–177.

[14] Seiser, R., Pitsch, H., Seshadri, K., Pitz, W. J., and Curran, H. J., "Extinction and Autoignition of n-Heptane in Counterflow Configuration," *Proceedings of the Combustion Institute*, Vol. 28, 2000, pp. 2029–2037.

[15] Lindstedt, R. P., and Maurice, L. Q., "Detailed Kinetic Modeling of n-Heptane Combustion," *Combustion Science and Technology*, Vol. 107, 1995, pp. 317–353.

[16] Fournet, R., Warth, V., Glaude, P. A., Battin-Leclerc, F., Scacchi, G., and Come, G. M., *International Journal of Chemical Kinetics*, Vol. 32, No. 1, 2000, pp. 36–51.

[17] Come, G. M., Warth, V., Glaude, P. A., Fournet, R., Battin-Leclerc, F., and Scacchi, G., "Computer-Aided Design of Gas-Phase Oxidation Mechanisms—Application to the Modeling of n-Heptane and Iso-Octane Oxidation," *Proceedings of the Combustion Institute*, Vol. 26, 1996, pp. 755–762.

[18] Glaude, P. A., Warth, V., Fournet, R., Battin-Leclerc, F., Come, G. M., and Scacchi, G., "Modeling of n-heptane and Iso-Octane Gas-Phase Oxidation at Low Temperature by Using Computer-Aided Designed Mechanisms," *Bulletin Des Societes Chimiques Belges*, Vol. 106, No. 106, 1997, p. 343.

[19] El. Bakali, A. E., Delfau, J.-L., and Vovelle, C., "Kinetic Modeling of a Rich, Atmospheric Pressure, Premixed n-Heptane/O2/N2 Flame," *Combustion and Flame*, Vol. 118, 1999, pp. 381–389.

[20] Doute, C., Delfau, J.-L., and Vovelle, C., "Detailed Reaction Mechanisms for Low Pressure Premixed n-Heptane Flames," *Combustion Science and Technology*, Vol. 147, Nos. 1–6, 1999, pp. 61–109.

[21] Muller, U. C., Peters, N., and Linan, A., "Global Kinetics for n-Heptane Ignition at High Pressures," *Proceedings of the Combustion Institute*, Vol. 24, 1992, pp. 777–784.

[22] Bui-Pham, M., and Seshadri, K., "Comparison Between Experimental Measurements and Numerical Calculations of the Structure of Heptane Air Diffusion Flames," *Combustion Science and Technology*, Vol. 79, Nos. 4–6, 1991, pp. 293–310.

[23] Bollig, M., Pitsch, H., Hewson, J. C., and Seshadri, K., "Reduced n-Heptane Mechanism for Non-Premixed Combustion with Emphasis on Pollutant Relevant Intermediate Species," *Proceedings of the Combustion Institute*, Vol. 26, 1996, pp. 729–737.

[24] Chakir, A., Belliman, M., Boettner, J. C., and Cathonnet, M., "Kinetic Study of n-Heptane oxidation," *International Journal of Chemical Kinetics*, Vol. 24, No. 4, 1992, pp. 385–410.

[25] Ranzi, E., Gaffuri, P., Faravelli, T., and Dagaut, P., "A Wide-Range Modelling Study of n-Heptane Oxidation," *Combustion and Flame*, Vol. 103, Nos. 1–2, 1995, pp. 91–106.

[26] Callahan, C. V., Held, T. J., Dryer, F. L., Minetti, R., Ribaucour, M., Sochet, L. R., Faravelli, T., Gaffuri, P., and Ranzi, E., "Experimental Data and Kinetic Modeling of Primary Reference Fuel Mixtures," *Proceedings of the Combustion Institute*, Vol. 26, 1996, pp. 739–746.

[27] Darabiha, N., Lacas, F., Rolon, J. C., and Candel, S., "Laminar Counterflow Spray Diffusion Flames—A Comparison Between Experimental Results and Complex Chemistry Calculations," *Combustion and Flame*, Vol. 95, No. 3, 1993, pp. 261–275.

[28] Held, T. J., Marchese, A. J., and Dryer, F. L., "A Semi-Empirical Reaction Mechanism for n-Heptane Oxidation and Pyrolysis," *Combustion Science and Technology*, Vol. 123, Nos. 1–6, 1997, pp. 107–146.

[29] Ingermasson, A. T., Pedersen, J. R., and Olsson, J. O., "Oxidation of n-Heptane in a Premixed Laminar Flame," *Journal of Physical Chemistry A*, Vol. 103, No. 41, 1999, pp. 8222–8230.

[30] Basevich, V. Ya., Belyaev, A. A., Brandshteter, V., Neigauz, M. G., Tashl, R., and Frolov, S. M., "Simulation of Auto-Ignition of Isooctane and n-Heptane in an Internal-Combustion Engine," *Combustion, Explosion, and Shock Waves*, Vol. 30, No. 6, 1994, pp. 737–745.

[31] Coats, C. M., and Williams, A., "Investigation of the Ignition and Combustion of n-Heptane-Oxygen Mixtures," *Proceedings of the Combustion Institute*, Vol. 17, 1978, pp. 611–621.

[32] Gerstein, M., Levine, O., and Wong, E. L., "Flame Propagation. 2. The Determination of Fundamental Burning Velocities of Hydrocarbons by a Revised Tube Method," *Journal of the American Chemical Society*, Vol. 73, No. 1, 1951, pp. 418–422.

[33] Gibbs, G. J., and Calcote, H. F., "Effect of Molecular Structure on Burning Velocity," *Journal of Chemical and Engineering Data*, Vol. 4, No. 3, 1959, pp. 226–237.

---

*Data available online at http://www.me.berkeley.edu/gri_mech.

[34] Ciezki, H., and Adomeit, G., "Shock-Tube Investigation of Self-Ignition of n-Heptane Air Mixtures Under Engine Relevat Conditions," *Combustion and Flame*, Vol. 93, No. 4, 1993, pp. 421–433.

[35] Fieweger, K., Pfahl, U., Blumenthal, R., and Adomeit, G., "Motorische Verbrennung," *Kolloquium des Sonderforshungsbereich 224*, edited by F. Pishing, RWTH Aachen, 1996.

[36] Vermeer, D. J., Meyer, J. W., and Oppenheim, A. K., "Auto-Ignition of Hydrocarbons Behind Reflected Shock-Waves," *Combustion and Flame*, Vol. 18, No. 3, 1972, pp. 327–336.

[37] Adomeit, G., 1989.

[38] Burcat, A., Farmer, R. F., and Matula, R. A., *13th International Symposium on Shock Tubes and Waves*, edited by Ch. E. Treanor and J. G. Hall, 1981, pp. 826–833.

[39] Ciezki, H., and Adomeit, G., *16th International Symposium on Shock Tubes and Waves*, 1987, pp. 481–486.

[40] Poppe, C., Schreber, M., and Griffiths, J. F., *Proceedings of Joint Meeting of the Soviet and German Sections of the Combustion Institute*, Cambridge, 1993, p. 360.

[41] Teichmann, H., "Die Selbstentzundung von Kohlenwasserstoff-Luftgemishen und das Klopfen im Otto-Motor," *Zeitschrift fur Elektrochemie und Angewandte Physikalische Chemie*, Vol. 47, No. 4, 1941, pp. 297–307.

[42] Scheuermeyer, M., and Steigerwald, H., "Die Messung des Zundverzugs Verdichteter Kraftstoff-Luft-Gemische zur Untersuchung der Klopfneigung," *Motortechnische Zeitschrift*, Vol. 5, Nos. 8–9, 1943, pp. 224–235.

[43] Rogener, H., "Entzundung von Konlenwasserstoff-Luft-Gemischen Durch Adiabatische Verdichtung," *Zeitschrift fur Elektrochemie und Angewandte Physikalische Chemie*, Vol. 53, No. 6, 1949, pp. 389–397.

[44] Taylor, C. F., Taylor, E. S., Livengood, J. C., Russell, W. A., and Leary, W. A., "Ignition of Fuels by Rapid Compression," *SAE Quarterly Transactions*, Vol. 4, No. 2, 1950, pp. 232–270.

[45] Hamins, A., "Diffusion Flame Studies," Ph.D. Dissertation, Univ. of California, San Diego, 1985.

[46] Hamins, A., and Seshadri, K., "The Structure of Diffusion Flames Burning Pure, Binary and Ternary Solutions of Methanol, Heptane, and Toluene," *Combustion and Flame*, Vol. 68, No. 3, 1987, pp. 295–307.

[47] Abdel-Khalic, S. I., Tamaru, T., and El-Wakie, M., "A Chromatographic and Interferometric Study of the Diffusion Flame Around a Simulated Fuel Drop," *Proceedings of the Combustion Institute*, Vol. 15, 1968, pp. 389–399.

[48] Abdel-Khalic, S. I., "An Investigation of the Diffusion Flame Surrounding a Simulated Liquid Fuel Droplet," Ph.D. Dissertation, Univ. of Wisconsin, Madison, 1973.

[49] Kent, J. H., and Williams, F. A., "Extinction of Laminar Diffusion Flames for Liquid Fuels," *Proceedings of the Combustion Institute*, Vol. 15, 1974, pp. 315–325.

[50] Seshadri, K., Ph.D. Dissertation, Univ. of California, San Diego, 1977.

[51] Bakali, A. E., Delfau, J.-L., and Vovelle, C., "Experimental Study of 1 Atmosphere, Rich, Premixed n-Heptane and Iso-Octane Flames," *Combustion Science and Technology*, Vol. 140, Nos. 1–6, 1998, pp. 69–91.

[52] Doute, C., Delfau, J.-L., and Vovelle, C., "Experimental Study of the Chemical Structure of Low-Pressure Premixed n-Heptane-O_2-Ar and Iso-Octane-O_2-Ar Flames," *Combustion Science and Technology*, Vol. 124, Nos. 1–6, 1997, pp. 249–276.

[53] Dagaut, P., Reuillon, M., and Cathonnet, M., "High-Pressure Oxidation of Liquid Fuels from Low to High-Temperature 1, N-Heptane and Iso-Octane," *Combustion Science and Technology*, Vol. 95, Nos. 1–6, 1994, pp. 233–260.

[54] Dagaut, P., Reuillon, M., and Cathonnet, M., "Experimental Study of the Oxidation of n-Heptane in a Jet-Stirred Reactor from Low Temperature to High Temperature and Pressures up to 40 atm," *Combustion and Flame*, Vol. 101, Nos. 1–2, 1995, pp. 132–140.

[55] Dagaut, P., Boettner, J. C., and Cathonnet, M., "High Pressure Oxidation of Liquid Fuels from Low to High Temperature 2, Mixtures of n-Heptane and Isooctane," *Combustion Science and Technology*, Vol. 103, Nos. 1–6, 1994, pp. 315–336.

[56] Dagaut, P., Koch, R., and Cathonet, M., "The Oxidation of n-Heptane in the Presence of Oxygenated Octane Improvers: MTBE and ETBE," *Combustion Science and Technology*, Vol. 122, Nos. 1–6, 1997, pp. 345–361.

[57] Vermeersch, M. L., Held, T. J., Stein, Y. S., and Dryer, F. L., "Autoignition Chemistry Studies of n-Heptane in a Variable Pressure Flow Reactor," *SAE Transactions*, Vol. 100, No. 4, 1991, pp. 645–661.

[58] Barnard, J. A., and Harwood, B. A., "Spontaneous Combustion of Normal Heptane," *Combustion and Flame*, Vol. 21, No. 2, 1973, pp. 141–152.

[59] Minetti, R., Carlier, M., Ribaucour, M., Therssen, E., and Sochet, L. R., "A Rapid Compression Machine Investigation of Oxidation and Auto-Ignition of n-Heptane, Measurements and Modeling," *Combustion and Flame*, Vol. 102, No. 3, 1995, pp. 298–309.

[60] Minetti, R., Carlier, M., Ribaucour, M., Therssen, E., and Sochet, L. R., "Comparison of Oxidation and Autoignition of the two Primary Reference Fuels by Rapid Compression," *Proceedings of the Combustion Institute*, Vol. 26, 1996, pp. 747–753.

[61] Griffiths, J. F., Halford-Maw, P. A., and Rose, D. J., "Fundamental Features of Hydrocarbon Autoignition in a Rapid Compression Machine," *Combustion and Flame*, Vol. 95, No. 3, 1993, pp. 291–306.

[62] Griffiths, J. F., Hughes, K. J., Schreiber, M., and Poppe, C., "An Unified Approach to the Reduced Kinetic Modeling of Alkane Combustion," *Combustion and Flame*, Vol. 99, Nos. 3–4, 1994, pp. 533–540.

[63] Cox, A., Griffiths, J. F., Mohamed, C., Curran, H., Pitz, W. J., and Westbrook, C. K., "Extents of Alkane Combustion During Rapid Compression Leading to Single- and Two-Stage Ignition," *Proceedings of the Combustion Institute*, Vol. 26, 1996, pp. 2685–2692.

[64] Leppard, W. R., 1987.

[65] Warnatz, J., "Chemistry of High Temperature Combustion of Alkanes up to Octane," *Proceedings of the Combustion Institute*, Vol. 20, 1984, pp. 845–856.

[66] Westbrook, C. K., Pitz, W. J., Curran, H. C., Boercker, J., and Kunrath, E., "Chemical Kinetic Modeling Study of Shock Tube Ignition of Heptane Isomers," *International Journal of Chemical Kinetics*, Vol. 33, No. 12, 2001, pp. 868–877.

[67] Westbrook, C. K., Pitz, W. J., Boercker, J. E., Curran, H. J., Griffiths, J. F., Mohamed, C., and Ribaucour, M., "Detailed Chemical Kinetic Reaction Mechanisms for Autoignition of Isomers of Heptane Under Rapid Compression," *Proceedings of the Combustion Institute*, Vol. 29, Pt. 1, 2002, pp. 1311–1318.

[68] Chakir, A., Cathonnet, M., Boettner, J. C., and Gaillard, F., "Kinetic Study of n-Butane Oxidation," *Combustion Science and Technology*, Vol. 65, Nos. 4–6, 1989, pp. 207–230.

[69] Chakir, A., Cathonnet, M., Boettner, J. C., and Gaillard, F., "Kinetic Study of 1-Butene Oxidation in a Jet-Stirred Flow Reactor," *Proceedings of the Combustion Institute*, Vol. 22, 1988, pp. 873–881.

[70] Dagaut, P., Boettner, J. C., Cathonnet, M., and Gaillard, F., "Kinetic Modeling of Propane Oxidation," *Combustion Science and Technology*, Vol. 56, Nos. 1–3, 1987, pp. 23–63.

[71] Dagaut, P., Cathonnet, M., and Boettner, J. C., "Propyne Oxidation - A Kinetic Modeling Study," *Combustion Science and Technology*, Vol. 71, Nos. 1–3, 1990, pp. 111–128.

[72] Dagaut, P., Cathonnet, M., and Boettner, J. C., "Kinetics of Ethane Oxidation," *International Journal Chemical Kinetics*, Vol. 23, No. 5, 1991, pp. 437–455.

[73] Foelshe, R. O., Keen, J. M., and Solomon, W. C. "A Non-Equilibrium Computational Method for Predicting Fuel Rich Gas Generator Performance and Exhaust Properties. Vol. 2: Reaction Kinetics and Computational Results," Univ. of Illinois, Rept. AAE9307, UIL93-0507, Urbana, 1993.

[74] Tsang, W., "Thermal Stability of Cyclohexane and 1-Hexene," *International Journal of Chemical Kinetics*, Vol. 10, No. 11, 1978, pp. 1119–1138.

[75] Tsang, W., "Thermal Decomposition of Cyclopentane and Related Compounds," *International Journal of Chemical Kinetics*, Vol. 10, No. 6, 1978, pp. 599–617.

[76] Westbrook, C. K., Pitz, W. J., Thornton, M. M., and Malte, P. C., "A Kinetic Modeling Study of Normal Pentane Oxidation in a Well-Stirred Reactor," *Combustion and Flame*, Vol. 72, No. 1, 1988, pp. 45–62.

[77] Heimel, S., and Weast, R. C., "Effect of Initial Mixture Temperature on the Burning Velocity of Benzene-Air, n-Heptane-Air and Isooctane-Air Mixtures," *Proceedings of the Combustion Institute*, Vol. 6, 1956, pp. 296–302.

[78] Davis, S. G., and Law, C. K., "Determination of and Fuel Structure Effects on Laminar Flame Speeds of C1-C8 Hydrocarbons," *Combustion Science and Technology*, Vol. 140, Nos.1–6, 1998, pp. 427–449.

[79] Takahashi, K., Inomata, T., Abe, T., Fukaya, H., Hayashi, E., and Ono, T., "Inhibition of Combustion by Bromine-free Polyfluorocarbons. 2. Burning Velocities of Methane and n-Heptane Flames with Polyfluorocarbons containing Oxygen, Nitrogen, or Sulfur," *Combustion Science and Technology*, Vol. 131, Nos. 1–6, 1998, pp. 187–191.

[80] Babkin, V. S., V'yun, A. V., and Kozachenko, L. S., "Determination of Burning Velocity from Pressure Record in a Constant Volume Bomb," *Combustion, Explosion and Shock Waves*, Vol. 3, No. 3, 1967, pp. 221–225.

[81] Ryan, T. W., and Lestz, S. S., "The Laminar Burning Velocityu of Isooctane, n-Heptane, Methanol, Methane, and Propane at Elevated Temperature and Pressures in the Presence of a Diluent," SAE Preprints, No. 800103, 1980, p. 14.

[82] Hughes, K. J., Turanyi, T., Clague, A. R., and Pilling, M. J., "Development and Testing of a Comprehensive Chemical Mechanism for the Oxidation of Methane," *International Journal of Chemical Kinetics*, Vol. 33, No. 9, 2001, pp. 513–538, URL: http://www.chem.leeds.ac.uk/Combustion.html.

[83] Baulch, D. L., Cobos, C. J., Cox, R. A., Frank, P., Hayman, J., Just, T., Kerr, J. A., Murrells, T., Pilling, M. J., Troe, J., Walker, R. W., and Warnatz, J., "Evaluated Kinetic Data for Combustion Modeling. Supplement 1," *Journal of Physical and Chemical Reference Data*, Vol. 23, No. 6, 1994, pp. 847–1033.

[84] Mokrushin, V., and Tsang, W., "A Calculational Data Base for Unimolecular Reactions," *Abstracts of Work-in-Progress, 27th International Symposium on Combustion*, 1998, p. 439.

[85] Sumathi, R., Carstensen, H.-H., and Green, W. H., Jr., "Reaction Rate Prediction via Group Additivity. Part 2: H-Abstraction from Alkenes, Alkynes, Alcohols, Aldehydes, and Acids by H Atoms," *Journal of Physical Chemistry*, A, Vol. 105, No. 39, 2001, pp. 8969–8984.

[86] Qin, Z., Lissianski, V. V., Yang, H., Gardiner, W. C., Jr., Davis, S. G., and Wang, H., "Combustion Chemistry of Propane: A Case Study of Detailed Reaction Mechanism Optimization," *Proceedings of the Combustion Institute*, Vol. 28, 2000, pp. 1663–1669.

[87] Stein, S. E., Rukkers, J. M., and Brown, R. L., "NIST Structures & Properties Database and Estimation Program," National Inst. of Standards and Technology, Gaithersburg, MD, 1991.

[88] Stein, S. E., and Fahr, A., "High-Temperature Stabilities of Hydrocarbons," *Journal of Physical Chemistry*, Vol. 89, No. 17, 1985, pp. 3714–3725.

[89] Wang, H., and Frenklach, M., "Enthalpies of Formation of Benzenoid Aromatic Molecules and Radicals," *Journal of Physical Chemistry*, Vol. 97, No. 15, 1993, pp. 3867–3874.

[90] Kee, R. J., Rupley, F. M., and Miller, J. A., "CHEMKIN-II: A Fortran Chemical Kinetics Package for the Analysis of Gas Phase Chemical Kinetics," Sandia National Lab., SAND89-8009B, NM, 1989.

[91] Vermeer, D. J., Meyer, J. W., and Oppenheim, A. K., "Auto-Ignition of Hydrocarbons Behind Reflected Shock Waves," *Combustion and Flame*, Vol. 18, No. 3, 1972, pp. 327–336.

[92] Horning, D. C., Davidson, D. E., and Hanson, R. K., "Study of the High-Temperature Autoignition of n-Alkane/O2/Ar Mixtures," *Journal of Propulsion and Power*, Vol. 18, No. 2, 2002, pp. 363–371.

[93] Davidson, D. F., Herbon, J. T., Horning, D. C., and Hanson, R. K., "OH Concentration Time Histories in n-Alkane Oxidation," *International Journal of Chemical Kinetics*, Vol. 33, No. 12, 2001, pp. 775–783.

[94] Warnatz, J., "Resolution of Gas Phase and Surface Combustion Chemistry into Elementary Reactions," *Proceedings of the Combustion Institute*, Vol. 24, 1992, pp. 553–579.

[95] Westmoreland, P. R., "Thermochemistry and Kinetics of C2H3 + O2 Reactions," *Combustion Science and Technology*, Vol. 82, 1992, pp. 151–168.

[96] Mebel, A. M., Diau, E. W. G., Lin, M. C., and Morokuma, K., "Ab Initio and RRKM Calculations for Multichannel Rate Constants of the C2H3 + O2 Reaction," *Journal of the American Chemical Society*, Vol. 118, No. 40, 1996, pp. 9759–9771.

[97] Bozzelli, J. W., and Dean, A. M., "Hydrocarbon Radical Reactions with O2—Comparison of Allyl, Formyl, and Vinyl to Ethyl," *Journal of Physical Chemistry*, Vol. 97, No. 17, 1993, pp. 4427–4441.

[98] Carriere, T., Westmoreland, P. R., Kazakov, A., Stein, Y. S., and Dryer, F. L., "Modeling Ethylene Combustion from Low to High Pressure," *Proceedings of the Combustion Institute*, Vol. 29, Pt. 1, 2002, pp. 1257–1266.

[99] Fahr, A., and Laufer, A. H., "Ultraviolet Absorption of the Vinyl Radical and Reaction with Oxygen," *Journal of Physical Chemistry*, Vol. 92, No. 26, 1988, pp. 7229–7232.

[100] Knyazev, V. D., and Slagle, I. R., "Kinetics of the Reaction of Vinyl Radical with Molecular Oxygen," *Journal of Physical Chemistry*, Vol. 99, No. 8, 1995, pp. 2247–2249.

[101] Glassmann, I., *Combustion*, Academic Press, San Diego, CA, 1996.

[102] Pope, C. J., and Miller, J. A., "Exploring Old and New Benzene Formation Pathways in Low-Pressure Premixed Flames of Aliphatic Fuels," *Proceedings of the Combustion Institute*, Vol. 28, 2000, pp. 1519–1527.

[103] Babushok, V., and Tsang, W., "Inhibitor Rankings for Alkane Combustion," *Combustion and Flame*, Vol. 123, No. 4, 2000, pp. 488–506.